

SUPPLEMENTARY INFORMATION

for

Magnetoelastic coupling in the stretched diamond lattice of TbTaO₄

Xiaotian Zhang,^{*a} Nicola D. Kelly,^{ab} Denis Sheptyakov,^c Cheng Liu,^a Shiyu Deng,^{ad}

Siddharth S. Saxena^{*a} and Siân E. Dutton ^{*a}

^a Cavendish Laboratory, University of Cambridge, JJ Thomson Avenue, Cambridge, CB3 0HE, United Kingdom.

^b Department of Chemistry, University of Oxford, Mansfield Rd, Oxford OX1 3TA, United Kingdom.

^c Laboratory for Neutron Scattering and Imaging, Paul Scherrer Institut (PSI), Forschungsstrasse 111, 5232 Villigen PSI, Switzerland.

^d Institut Laue-Langevin (ILL), 71 Avenue des Martyrs, 38000 Grenoble, France.

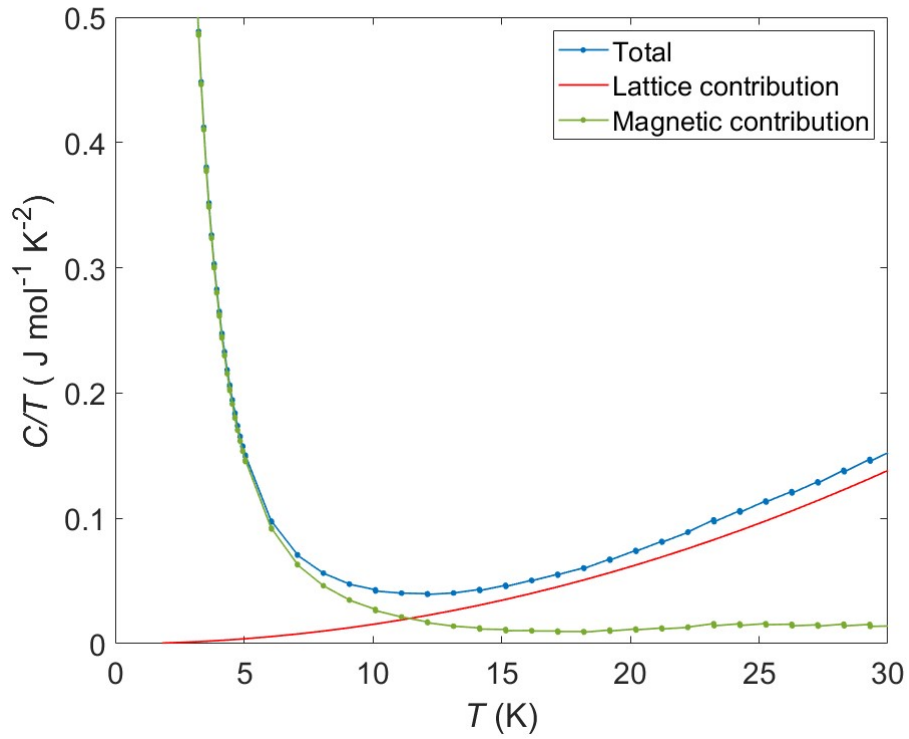


Fig. S1 Heat capacity data for $M\text{-TbTaO}_4$. Blue dots: total heat capacity (after subtraction of the Ag contribution from the raw data). Red line: Estimated lattice contribution using the Debye model with $\theta_d=370\text{ K}$. Green dots: magnetic contribution, $C_{mag}=C_{total}-C_{lattice}$.

Table S1: Refined Lattice parameters and atomic positions of $M\text{-TbTaO}_4$ from powder X-ray diffraction at room temperature. The O atomic positions were fixed at value from previous neutron diffraction data^{2,3}. Both Tb^{3+} and Ta^{5+} ions lie on (0.25, y , 0) sites.

Unit cell	
Space group	$I2/a$
$a/\text{Å}$	5.38264(15)
$b/\text{Å}$	11.0182(3)
$c/\text{Å}$	5.06692(13)
$\beta/^\circ$	95.6844(14)
Volume/ Å^3	299.025(14)
$R_{wp}/\%$	7.21
χ^2	2.10
Atomic positions	
yTb	0.6180 (3)
yTa	0.1502 (2)
$xO1$	0.090
$yO1$	0.461
$zO1$	0.252
$xO2$	-0.003
$yO2$	0.717
$zO2$	0.290

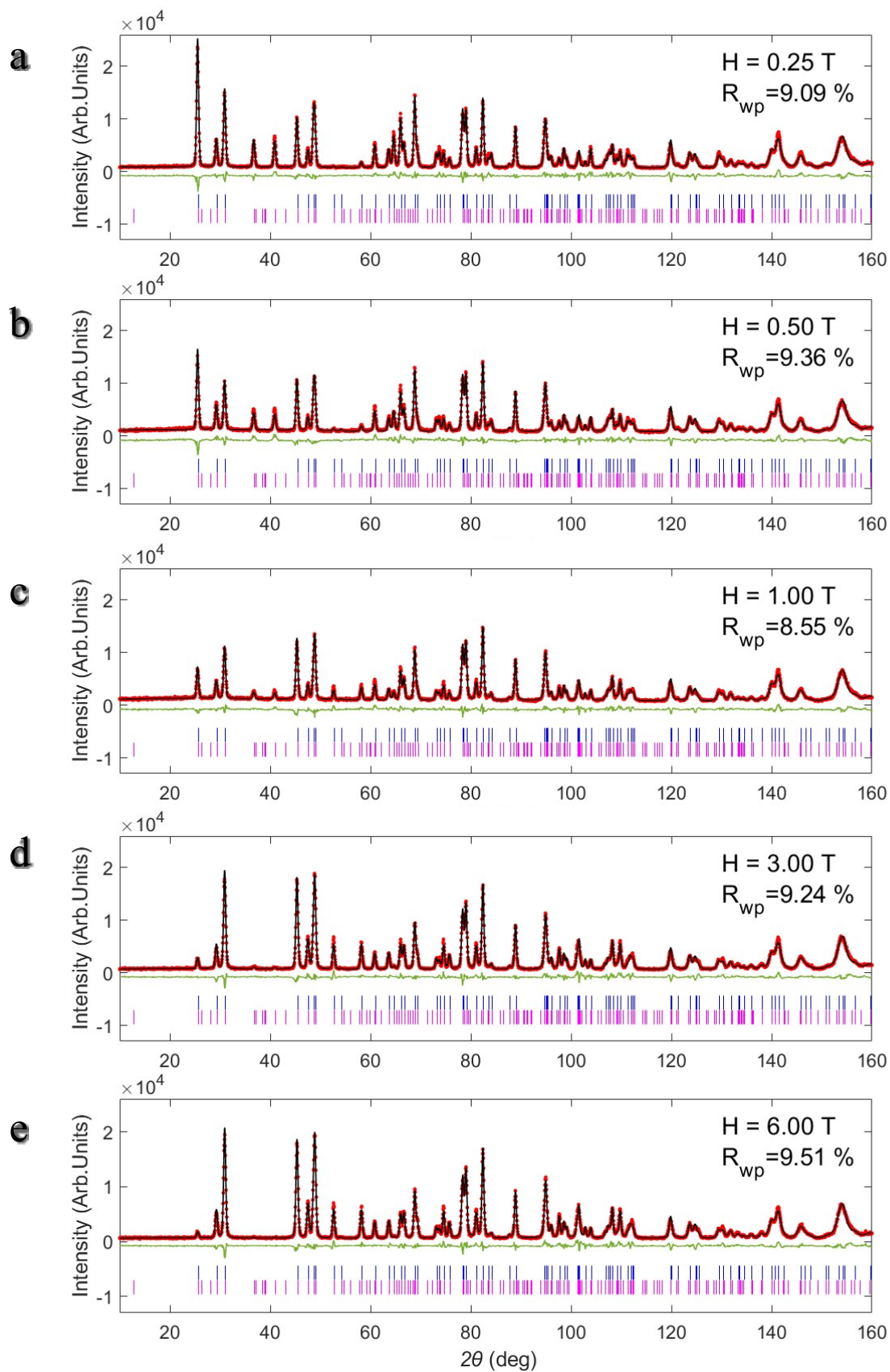


Fig. S2 (a-e) Refined PND data of $M\text{-TbTaO}_4$ collected at 1.6 K with 0.25 T, 0.50 T, 1 T, 3 T and 6 T. Red dots, experimental data; black line, calculated intensities; green line, difference pattern; tick marks, nuclear (blue), magnetic (pink) Bragg reflection positions.

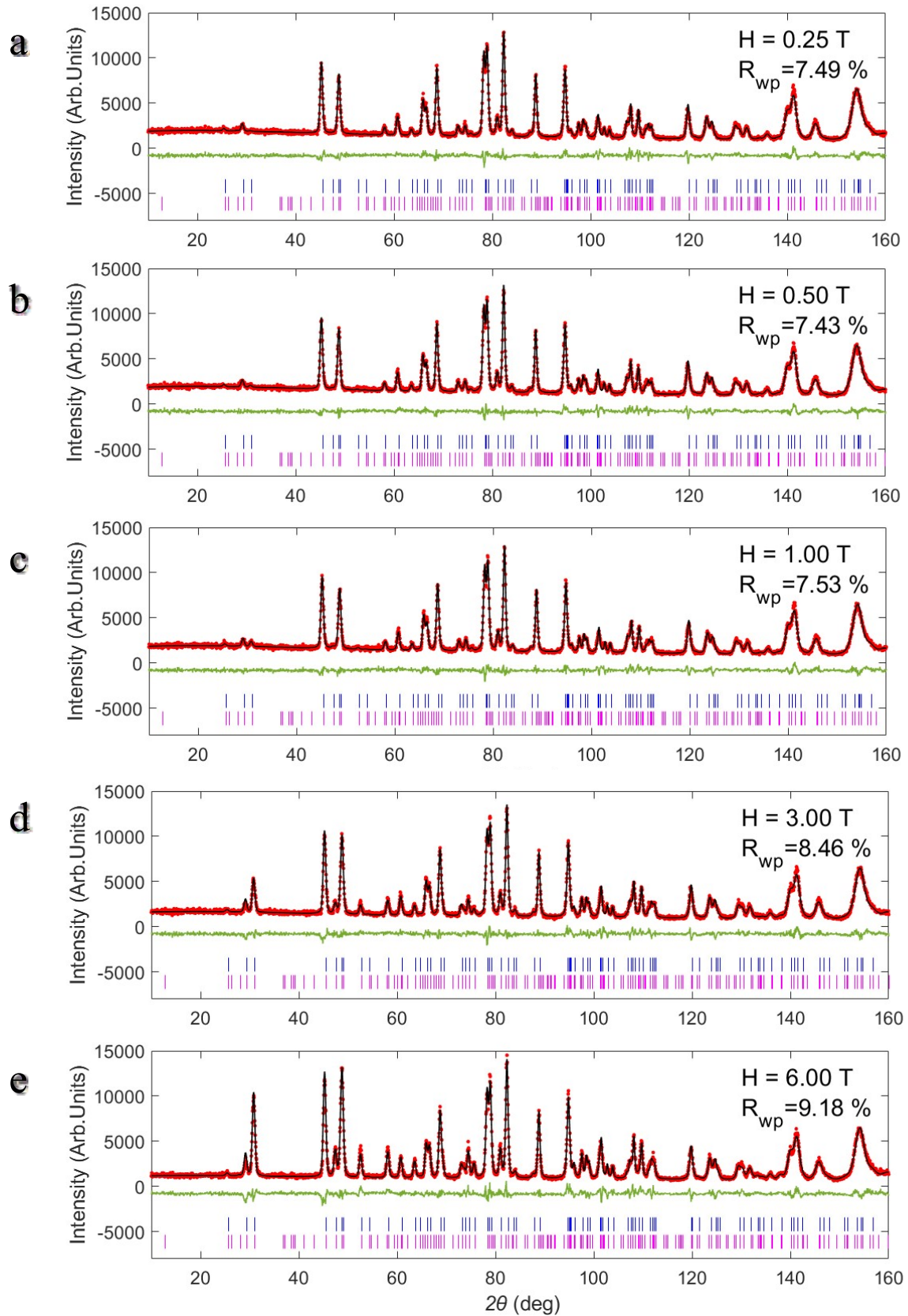


Fig. S3 (a-e) Refined PND data of $M\text{-TbTaO}_4$ collected at 20.0 K with 0.25 T, 0.50 T, 1 T, 3 T and 6 T. Red dots, experimental data; black line, calculated intensities; green line, difference pattern; tick marks, nuclear (blue), magnetic (pink) Bragg reflection positions.

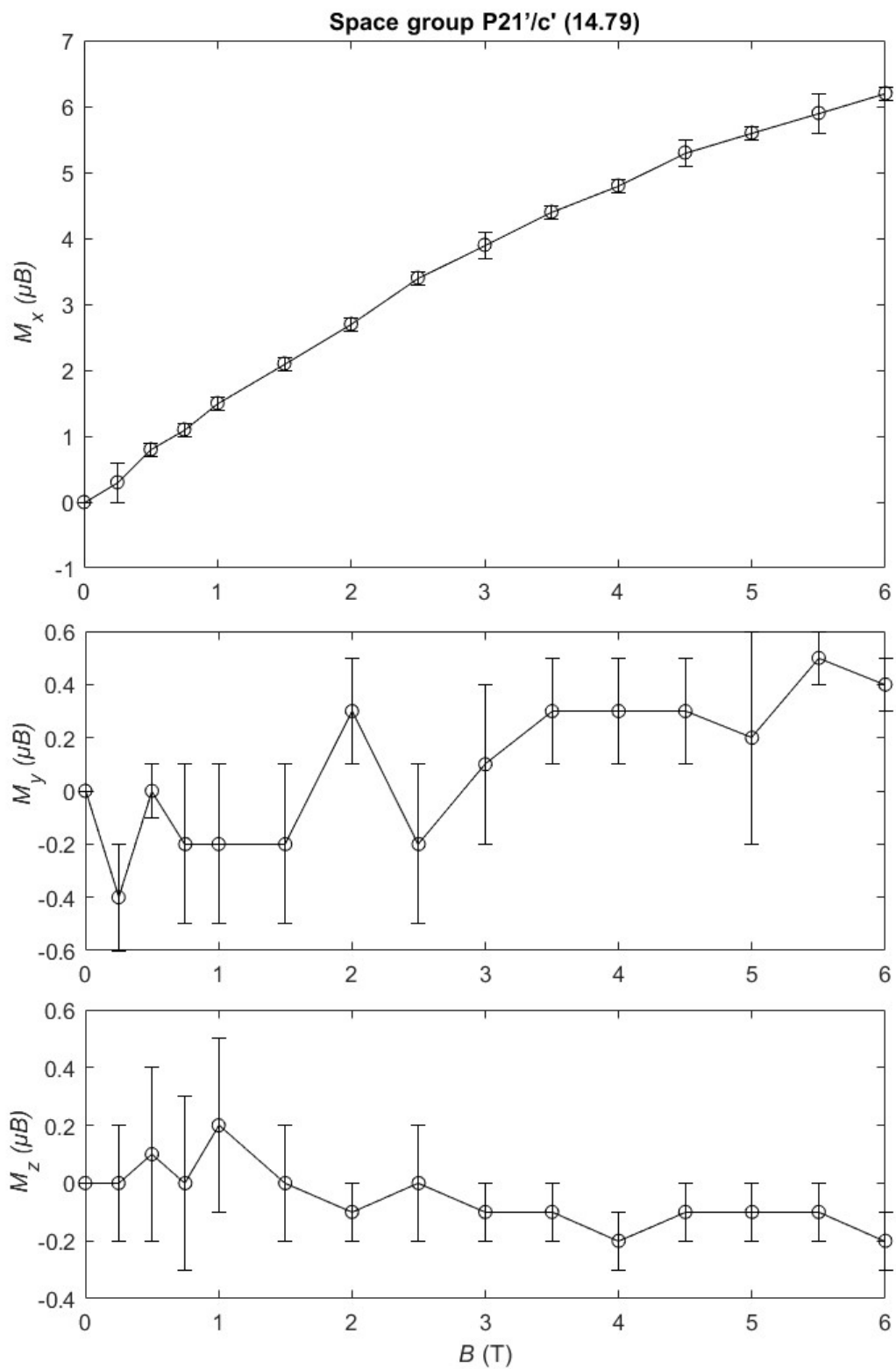


Fig. S4 Evolution of the Tb³⁺ lattice-coordinate magnetic moments along x, y and z axes as a function of magnetic field at 20.0 K from powder neutron diffraction (PND) data.

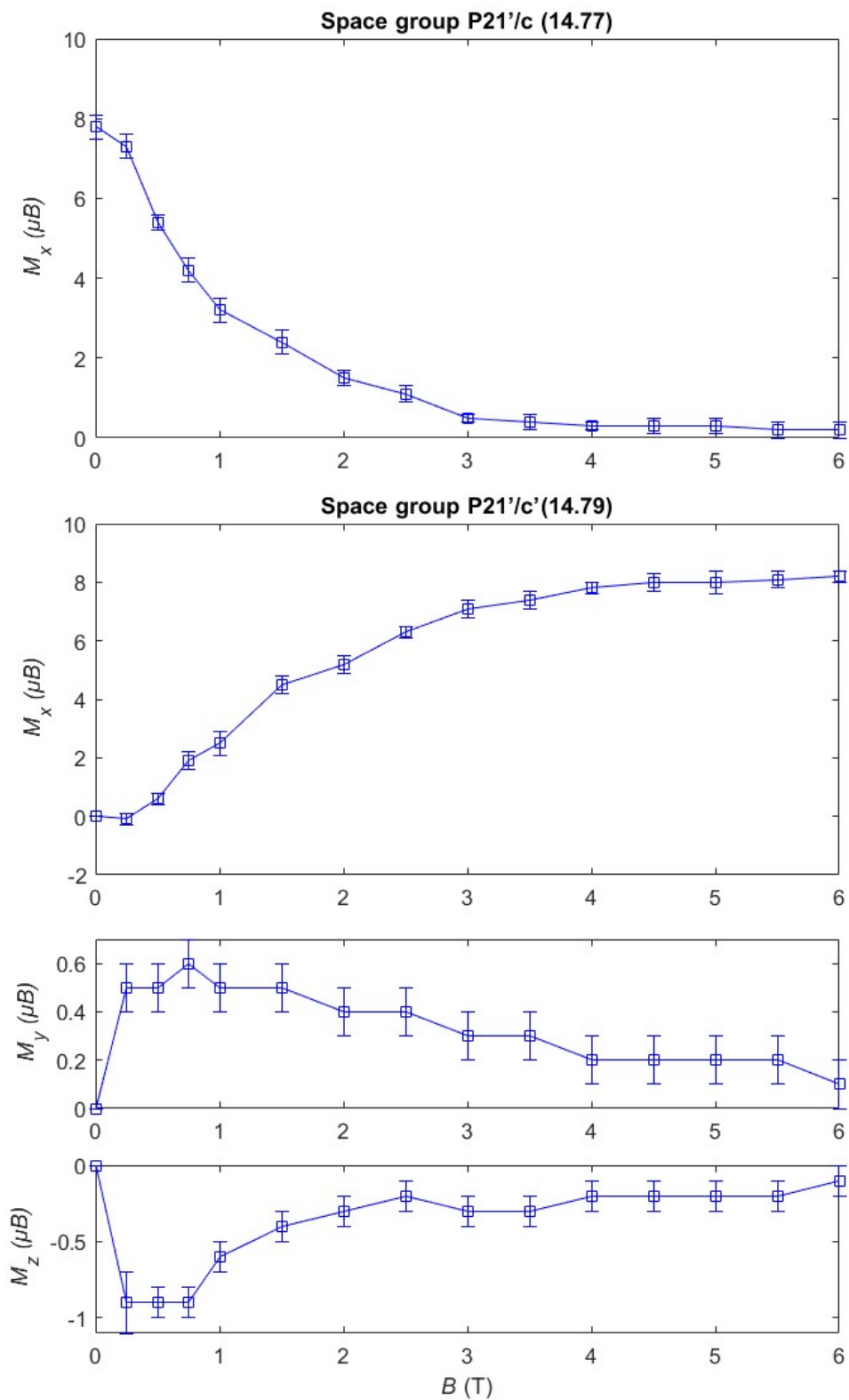
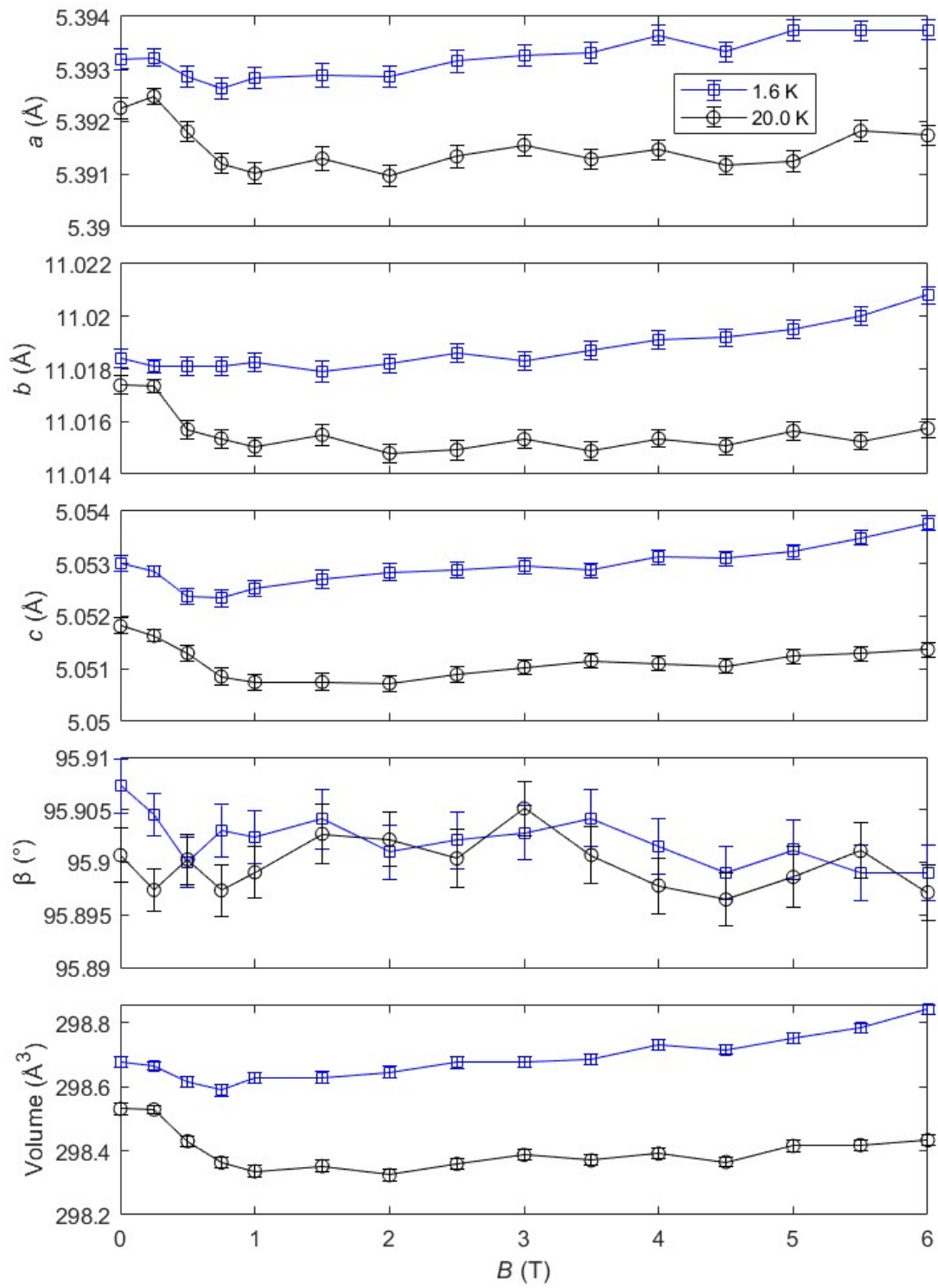


Fig. S5 Evolution of the Tb^{3+} lattice-coordinate magnetic moments along x, y and z axes as a function of magnetic field at 1.6 K from powder neutron diffraction (PND) data. The magnetic structure is modelled with a mixing of two magnetic space group. The phase fractions are fixed and identical to each other, while the magnetic moments are refined independently.



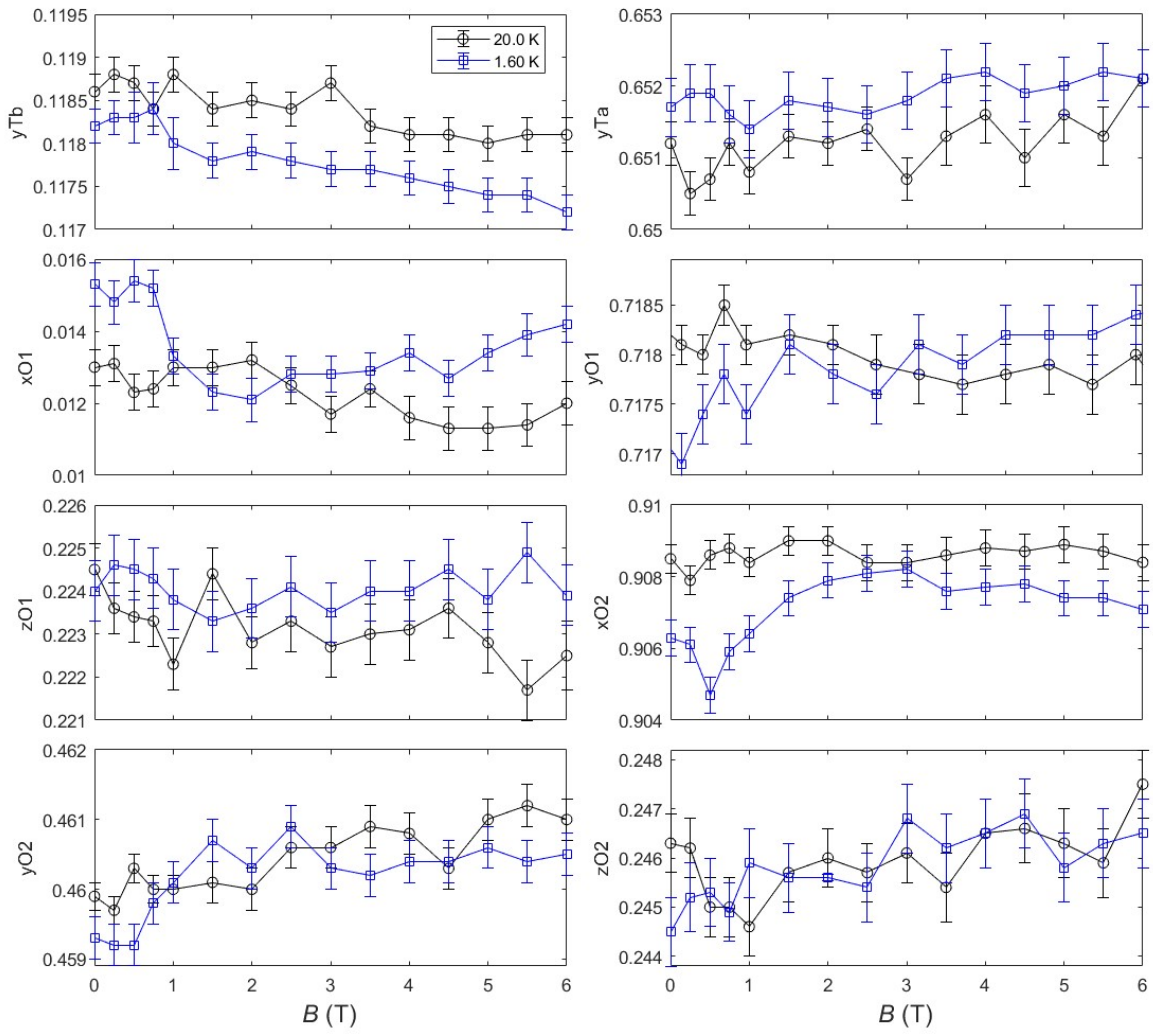


Fig. S7 Refined atomic positions of $M\text{-TbTaO}_4$ at 1.6 K and 20K as a function of magnetic field. Obtained from Rietveld refinement of powder neutron diffraction (PND) data collected on HRPT, PSI. $\lambda = 2.45 \text{ \AA}$.

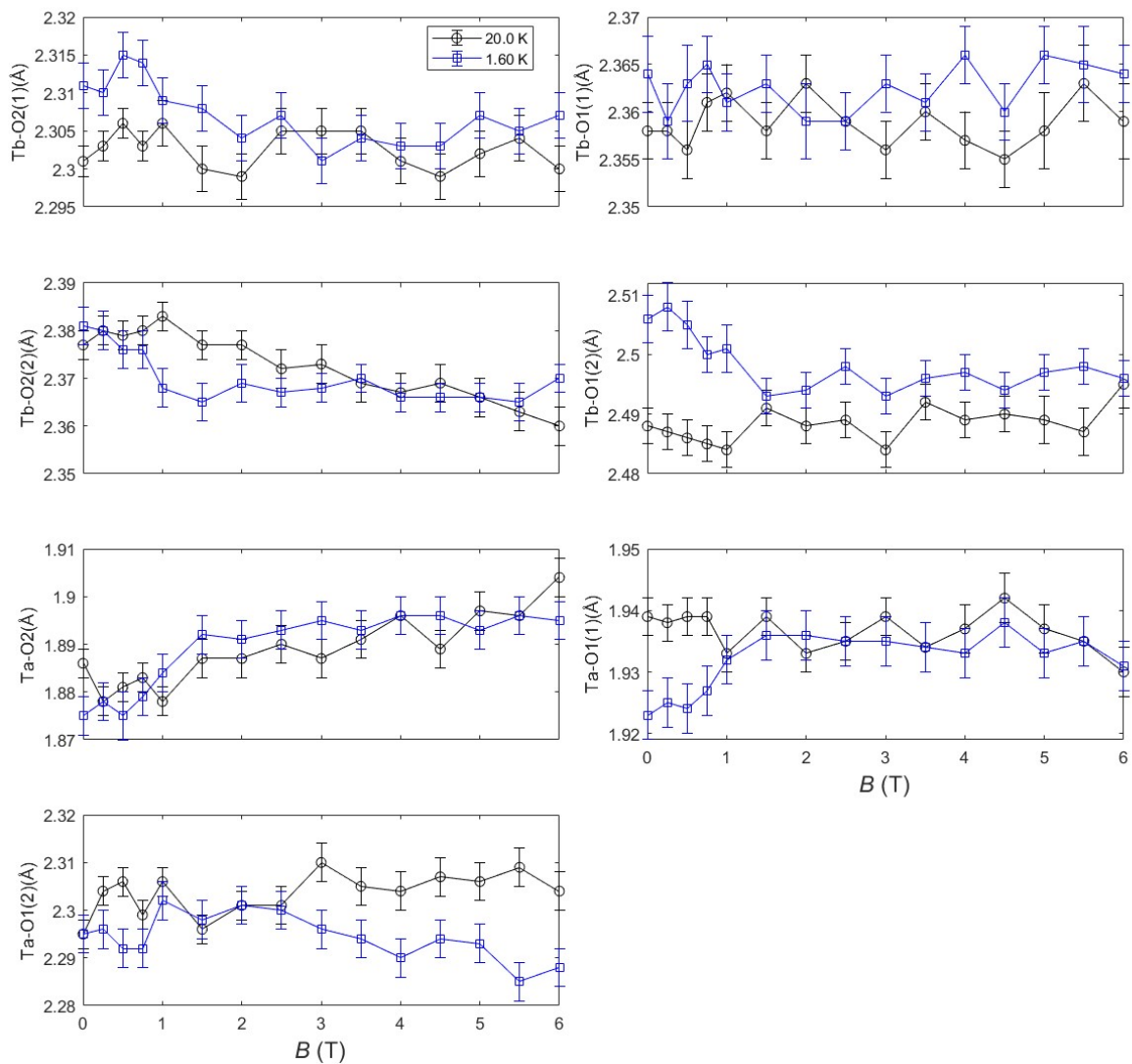


Fig. S8 Refined interatomic distances of $M\text{-TbTaO}_4$ at 1.6 K and 20K as a function of magnetic field. Obtained from Rietveld refinement of powder neutron diffraction (PND) data collected on HRPT, PSI. $\lambda = 2.45 \text{ \AA}$.

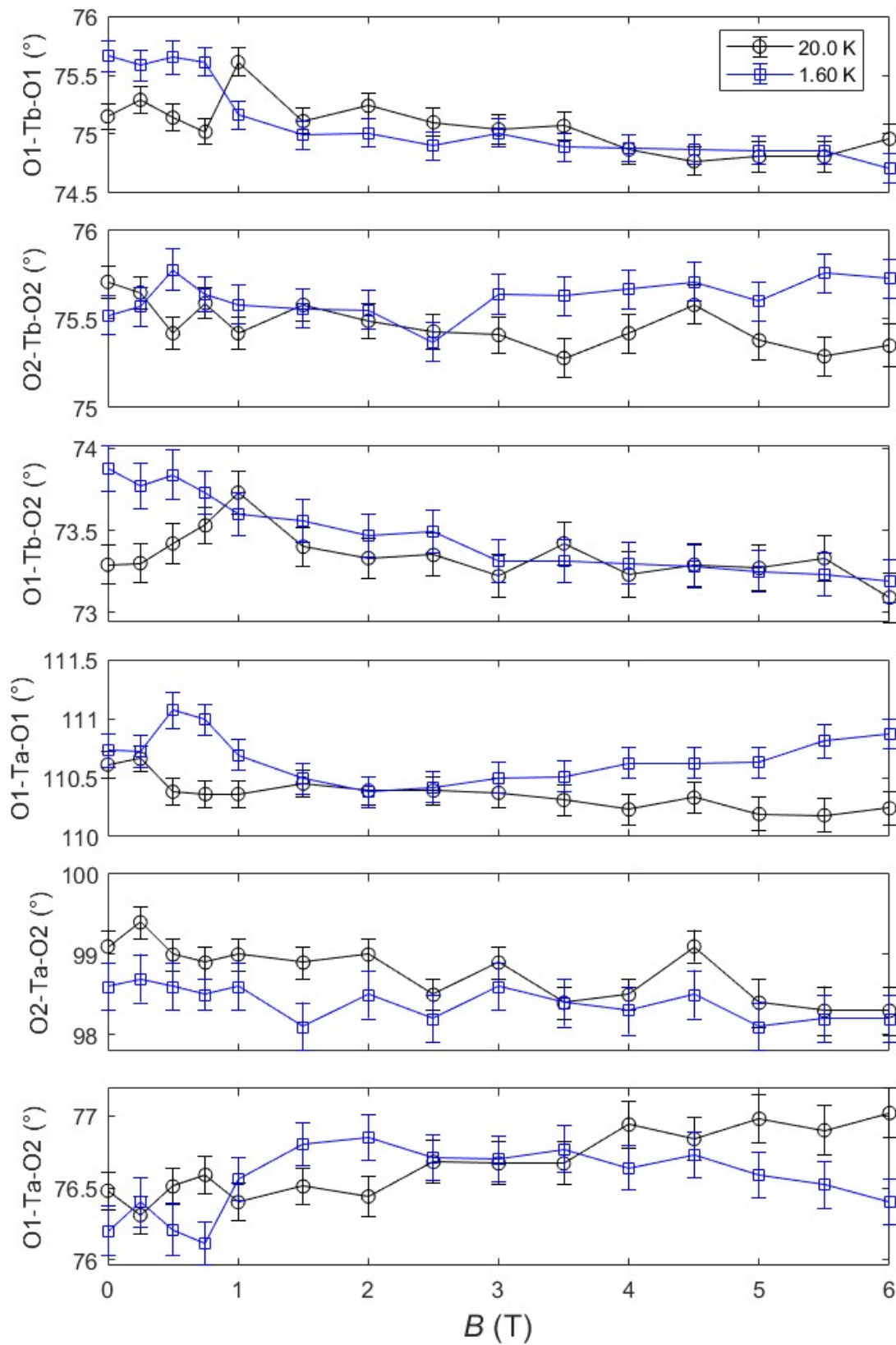


Fig. S9 Refined bond angles of $M\text{-TbTaO}_4$ at 1.6 K and 20K as a function of magnetic field. Obtained from Rietveld refinement of powder neutron diffraction (PND) data collected on HRPT, PSI. $\lambda = 2.45 \text{ \AA}$.

Reference

1. E. Gopal, *Specific heats at low temperatures*, Springer Science & Business Media, 2012.
2. N. D. Kelly, L. Yuan, R. L. Pearson, E. Suard, I. P. Orench and S. E. Dutton, *Phys Rev Mater*, 2022, **6**, 044410.
3. N. D. Kelly, C. V. Colin, S. E. Dutton, V. Nassif, I. P. Orench and E. Suard, *Institut Laue-Langevin*, 2021, DOI: 10.5291/ILL-DATA.5-31-2854.